Excitation Mechanisms of Whispering Gallery Modes with Direct Light Scattering

Xavier Zambrana-Puyalto,* Davide D'Ambrosio, and Gianluca Gagliardi

In optics, whispering gallery modes (WGMs) are modes of light that arise in cylindrically symmetric structures. Their intensity profile is strongly confined around the interface of the structure, and their Q-factors are some of the highest ever measured with light. Here, the physical mechanisms governing the coupling of a tangential beam into a WGM of a microsphere are analytically demonstrated. For that, Mie theory and the symmetries of light are made use of. It is demonstrated that the coupling mechanism is not related to any evanescent tunnelling effect. Rather, it is shown that it has to do with the angular momentum matching between the available inner WGMs of the sphere and the angular momentum content of the incident beam. The model is valid for any homogeneous sphere, for any wavelength, and for any incident cylindrically symmetric beam, focused or not. It quantitatively predicts the optical coupling efficiency to the resonator for any tangential position of the incident beam. And it sketches four different regimes of interaction depending on the beam position with respect to the sphere, properly matching experimental resonance spectra observed with free-space laser scattering.

1. Introduction

The study of optical resonances in microresonators is a well-established field with a great number of applications in lasers, quantum optomechanics, and sensing. These optical resonances are generally known as whispering gallery modes (WGMs)[1] or morphology-dependent resonances (MDR).[2] It is well accepted that a WGM mode is the first root $q = 1$ of a resonant multipolar mode with a large multipolar order j, and an azimuthal number $m = j$.[1] Although WGMs have a huge number of applications, a rigorous analytical description of the coupling mechanism between these resonant modes and the excitation field

Dr. X. Zambrana-Puyalto
Istituto Italiano di Tecnologia
Via Morego 30, Genova 16163, Italy
E-mail: xavislow@protonmail.com

Dr. X. Zambrana-Puyalto, Dr. D. D'Ambrosio, Dr. G. Gagliardi
Consiglio Nazionale delle Ricerche
Istituto Nazionale di Ottica (INO)
via Campi Flegrei 34—Comprensorio A. Olivetti, 80078 Pozzuoli (Na), Italy

(either in the form of off-axis Gaussian beam, or evanescent coupling) has never been given. In this article we study the excitation of WGMs with direct light, that is, the WGMs are excited with a focused off-axis Gaussian beam impinging on a dielectric sphere (e.g., a solid particle, a droplet). The state-of-the-art theoretical description of the coupling mechanism between a microsphere and a tangentially focused Gaussian beam is given in refs. [3–6]. In this particular description, it is intuitively understood that a portion of the incoming beam is evanescently transmitted to the interior of the particle. This light stays trapped inside of the particle and keeps reflecting back and forth. At resonance, the reflections are in phase with each other. Thus, the amplitude of the field increases very prominently inside the surface, and just outside of it. Part of this huge field amplitude escapes the sphere and can be detected in the far field. Note that the description above is based on scalar wave optics. However, in the state-of-the-art formal description, the vectorial Mie theory is used to compute the light–matter interaction. In this approach, the beam-shape coefficients for the tangential focused Gaussian beam are computed with the so-called localized approximation. The theory has been able to describe different experimental works, even those where the optical excitation was done by an evanescent field.[7,8] Yet, a fully rigorous analytical interpretation that reconciles the physical intuition with the vectorial analytical description still needs to be provided.

In this work, we set out to give an analytical explanation of the WGM coupling mechanism for the tangential free-space excitation scheme. To do that, we use Mie theory. We consider a Gaussian beam propagating along the z direction and focused with a lens with a certain numerical aperture (NA) (see **Figure 1**). The beam is focused onto the center of the particle. We compute the beam-shape coefficients of the focused Gaussian beam thanks to the semi-analytical formulas put forward in refs. [9–11]. The semi-analytical formalism is valid for any cylindrically symmetric beam. Then, we translate the beam a certain distance d along a certain direction $\mathbf{u}$. We compute the new beam-shape coefficients with respect to the new position. For a tangential excitation, we make $\mathbf{u} = \hat{\mathbf{y}}$. Because the initial beam has a linear momentum along the z axis and the displacement is along the y axis, then the beam acquires a non-negligible transverse AM content along the x axis.[12,13] In fact, we observe that the fundamental reason why an off-axis Gaussian can excite a WGM is the angular

**ADVANCED
SCIENCE NEWS**

www.advancedsciencenews.com
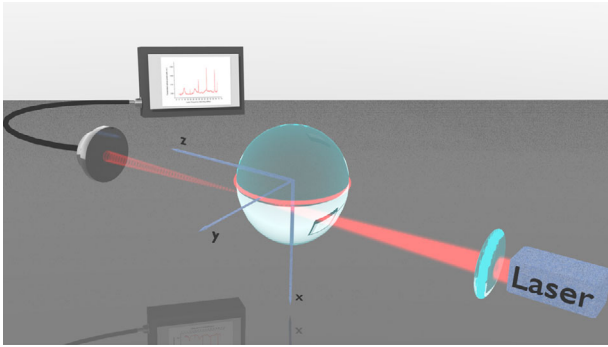
LASER
& PHOTONICS
REVIEWS

www.lpr-journal.org

Figure 1. Schematics of the problem. A cylindrically symmetric beam propagating along the z axis is displaced in the y direction. The beam, which is focused by a lens, tangentially hits the surface of a spherical microresonator and excites a WGM which revolves around the x axis.

momentum (AM) matching between the beam and the WGM of the sphere. Intuitively, the WGMs of a sphere of radius R and relative index of refraction n_r happen for multipolar modes of the order $j \gtrsim 2\pi R/\lambda$.[14] And thanks to the displacement $\mathbf{d} = d\hat{y}$, the beam gets an AM along the x axis $\langle J_x \rangle \approx 2\pi d/\lambda$. That means that the beam can couple to the WGMs with $m_x = j \gtrsim 2\pi R/\lambda$ when $d \approx R$. Our semi-analytical calculations allow us to calculate the exact coupling efficiency of the beam-WGM interaction for any $\lambda, R, n_r, d,$ NA. We differentiate between four interaction regimes, depending on their R/d value. Using an off-axis Gaussian beam focused with an NA = 0.4 and displaced by $d = 82\,\mu m$, we numerically sort them out as (see **Figure 2**):

1. $R < 0.93d$. In this regime, the interaction is null. The beam has been displaced too far apart from the sphere, and as a result there is no scattering.
2. $0.93d \leq R < 0.98d$. The axis of symmetry of the beam is outside of the surface of the sphere, yet the beam interacts with the particle through the tail of its transverse intensity distribution. The scattering is almost null except for a set of very sharp resonant conditions, which yield almost pure WGMs. The incident direction of the beam is not modified.
3. $0.98d \leq R < 1.01d$. The axis of symmetry of the beam is tangential or slightly inside/outside of the sphere. As a result, most of the beam (but not all), is blocked by the sphere. In this regime, the scattering is as large as it can get. The incident beam is heavily distorted by the sphere. The incident direction of the beam is modified, and some new relevant scattering directions pop up. Some WGMs are excited, but they are hidden under the superposition of lots of modes, thus making it difficult to observe them.
4. $R \geq 1.01d$. The whole beam is blocked by the sphere. The incident direction of the beam is completely modified by the sphere and steered toward another direction.

In Figure 2, we have plotted the scattering cross section σ^{sca} as a function of R/d to stress the fact that the four different regimes can always be found regardless of the wavelength of the laser, the size/material of the particle and the NA of the focusing lens. That is, $\lambda, R, n_r,$ NA affect the numeric R/d definition of the four regimes, but it does not affect their fundamental nature. After all, the nature of these four regimes is purely geometrical, and the geometry of the problem is defined by these four parameters.

Our semi-analytical calculations not only allow us to fully understand the mechanism behind WGM excitation with off-axis beams, but also they can be used to match the experimental data measured by some of the authors in previous works on liquid droplet microresonators.[15–19] Our results have huge implications in the field of microresonators, as they allow us to predict and characterize the exact WGMs that can be excited depending on the properties of the beam and its alignment. Note, though, that scope of this work is to develop a theoretical formalism. A separate work to demonstrate the match between our model and the experimental data is underway, and it will be presented elsewhere.

2. Theory

2.1. Generalized Lorenz–Mie Theory

We set out to theoretically describe the interaction problem between an off-axis focused Gaussian beam and a microresonator. A sketch of the problem that we are describing is shown in Figure 1. Unless explicitly mentioned otherwise, the wavelength is set to $\lambda = 640$ nm. We describe this interaction within the framework of Mie theory (also known as Generalized Lorenz–Mie Theory, GLMT[2]), which is one of the few analytical solutions of Maxwell equations. In Mie theory, the electromagnetic (EM) field ($\mathbf{E}^{tot}$) is divided into three: The incident field $\mathbf{E}^i$, the scattered field $\mathbf{E}^{sca}$, and the internal field $\mathbf{E}^{int}$. As a result, $\mathbf{E}^{tot} = \mathbf{E}^i + \mathbf{E}^{sca} + \mathbf{E}^{int}$. All three fields are expressed with respect to a reference frame that is placed in the center of the sphere. The key variable of the problem is $\mathbf{E}^i$. Experimentally, it is the easiest variable to manipulate. And theoretically, once the mathematical expression of $\mathbf{E}^i$ has been found, it is straightforward to find the expressions for $\mathbf{E}^{sca}$ and $\mathbf{E}^{int}$. Here, we are interested in finding the mathematical description of an off-axis focused Gaussian beam, yet the analytical description that will follow is valid for any cylindrically symmetric beam. To do that, first we obtain the multipolar decomposition of an on-axis focused cylindrically symmetric beam. And then, we apply a translation to the beam, and find the multipolar decomposition with respect to the initial (nondisplaced) reference frame. That is, we express all our results with respect to a multipolar basis[20–22] centred at center of the sphere. We express the multipolar basis as $\{\mathbf{A}_{jm_z}^{(\gamma)}\}$, with $(\gamma) = (e)$ being the electric multipoles and $(\gamma) = (m)$ the magnetic ones. $\mathbf{A}_{jm_z}^{(\gamma)}$ are eigenstates of the operators: AM squared (J^2), the projection of the AM momentum operator along the z axis (J_z), and parity Π. Their eigenvalues are $J^2\mathbf{A}_{jm_z}^{(\gamma)} = j(j+1)\mathbf{A}_{jm_z}^{(\gamma)}$, $J_z\mathbf{A}_{jm_z}^{(\gamma)} = m_z\mathbf{A}_{jm_z}^{(\gamma)}$, $\Pi\mathbf{A}_{jm_z}^{(e)} = (-1)^j\mathbf{A}_{jm_z}^{(e)}$, and $\Pi\mathbf{A}_{jm_z}^{(m)} = (-1)^{j+1}\mathbf{A}_{jm_z}^{(m)}$. Then, a general incident beam can be decomposed into multipoles as $\mathbf{E}^i = \sum_{j=1}^{\infty} \sum_{m_z=-j}^{j} \alpha_{j,m_z}^{(e)} \mathbf{A}_{jm_z}^{(e)} + \alpha_{j,m_z}^{(m)} \mathbf{A}_{jm_z}^{(m)}$, where $\alpha_{j,m_z}^{(\gamma)}$ are the so-called beam-shape coefficients.[2] As mentioned before, once the expression of the incident beam is known, it is straightforward to find the expression of the scattered and internal field. The solution of the problem is expressed in the next equations

$$\mathbf{E}^i = \sum_{j=1}^{\infty} \sum_{m_z=-j}^{j} \alpha_{j,m_z}^{(e)} \mathbf{A}_{jm_z}^{(e)} + \alpha_{j,m_z}^{(m)} \mathbf{A}_{jm_z}^{(m)} \tag{1}$$
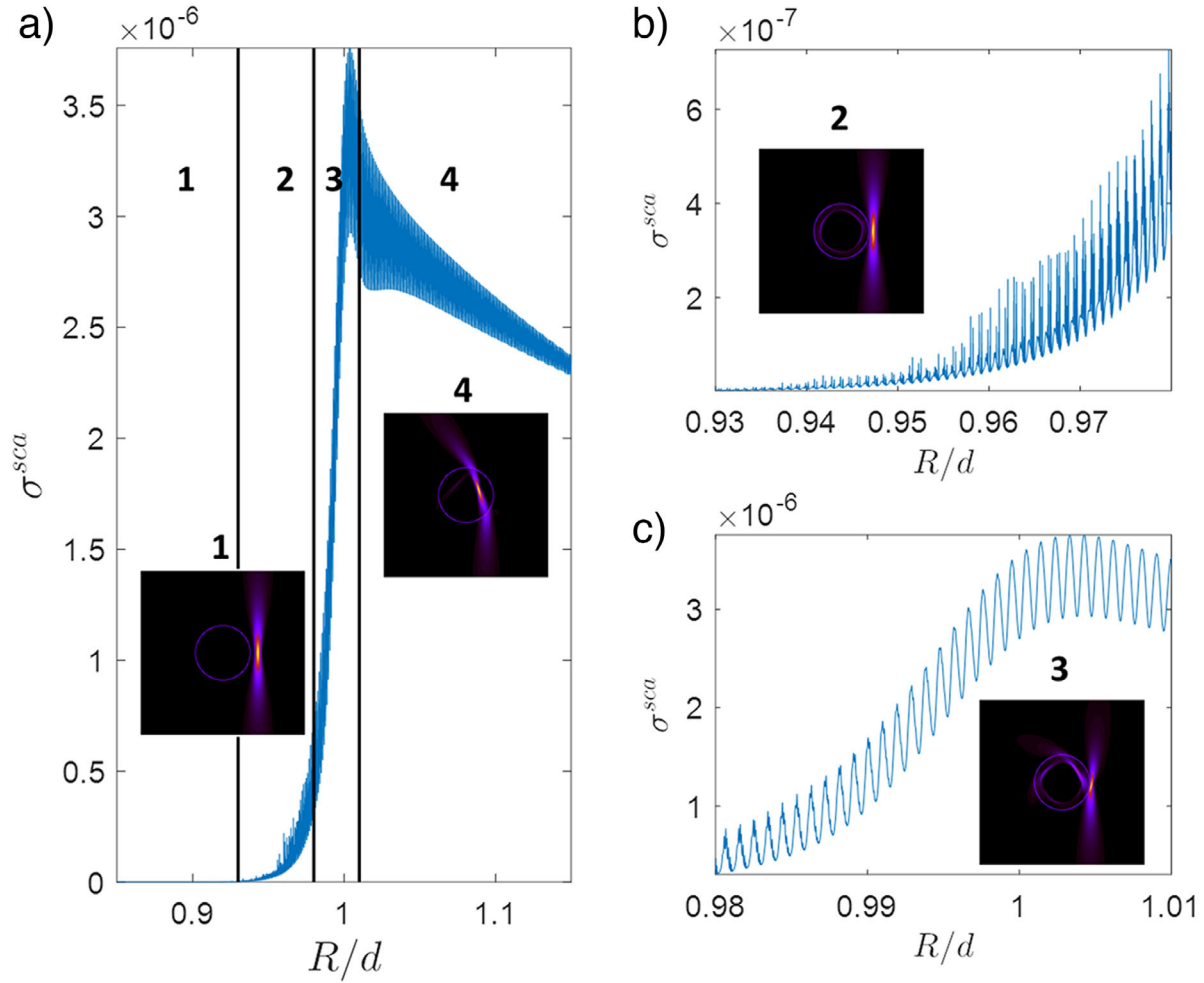
Figure 2. Regimes of interaction depending on the R/d ratio, where R is the radius of the particle and d is the beam displacement from the center of sphere. The cross section σ^{sca} plots are done for an incident left circularly polarized Gaussian beam displaced at $d = 82$ μm. The insets are $|\mathbf{E}^{tot}|^2$ plots in the $x = 0$ plane (see Figure 1) for a window of $3R \times 3R$ centred on the sphere. For all the plots, $\lambda = 640$ nm and NA $= 0.4$.

$$\mathbf{E}^{sca} = \sum_{j=1}^{\infty} \sum_{m_z=-j}^{j} \alpha_{j,m_z}^{(e)} a_j \mathbf{A}_{jm_z}^{(e)} + \alpha_{j,m_z}^{(m)} b_j \mathbf{A}_{jm_z}^{(m)} \qquad (2)$$

$$\mathbf{E}^{int} = \sum_{j=1}^{\infty} \sum_{m_z=-j}^{j} \alpha_{j,m_z}^{(e)} d_j \mathbf{A}_{jm_z}^{(e)} + \alpha_{j,m_z}^{(m)} c_j \mathbf{A}_{jm_z}^{(m)} \qquad (3)$$

where $\{a_j, b_j, c_j, d_j\}$ are the so-called Mie coefficients.[11,23] For the rest of this work, we only consider incident beams which are eigenstates of the helicity operator Λ.[11,24–27] The case is as general as any other, as any beam can be expressed as a superposition of the two different helicity components of light. Notice that a left (right) circularly polarized collimated beam is an eigenstate of $\Lambda = +1(-1)$. Then, as explained in refs. [9, 11, 28], the aplanatic model of a lens conserves the helicity of the incident collimated beam. As a result, a collimated beam which is an eigenstate of Λ (it is circularly polarized) remains an eigenstate of Λ after being focused by a lens or a microscope objective (MO). Note that focusing preserves helicity, but it does not preserve polarization: It is well known that tightly focused beams cannot be circularly polarized at the focal plane.[28,29] Then, we can

express a general focused beam with a well-defined helicity as $\mathbf{E}^i = \sum_{j=1}^{\infty} \sum_{m_z=-j}^{j} C_{j,m_z,p}^{on}(\mathbf{A}_{jm_z}^{(e)} + p\mathbf{A}_{jm_z}^{(m)})$, where $p = \pm 1$ is the helicity of the beam and $C_{j,m_z,p}^{on}$ is the beam-shape function. We say that a state has a *well-defined helicity* when it is an eigenstate of the helicity operator Λ. The expression of $C_{j,m_z,p}^{on}$ can be found in refs. [9, 11]. When the beam is cylindrically symmetric, that is, it is an eigenstate of J_z with value m_z^*, then the previous equation is reduced to

$$\mathbf{E}^i = \sum_{j=|m_z^*|}^{\infty} C_{j,m_z^*,p}^{on} \left(\mathbf{A}_{jm_z^*}^{(e)} + p\mathbf{A}_{jm_z^*}^{(m)} \right) \qquad (4)$$

As is explained in refs. [9, 11], $C_{j,m_z^*,p}^{on}$ can be tailored with m_z^* and with the NA of the lens. In short, for a given beam with (m_z^*, p), an increase in the NA results in a compression of the multipolar decomposition into a few modes. This is observed in **Figure 3**. The multipolar decompositions in the top row are obtained with an NA $= 0.9$, and compared to ones at the bottom, which are obtained with an NA $= 0.4$, they yield many less multipolar orders. Then, given a beam with helicity p and focused
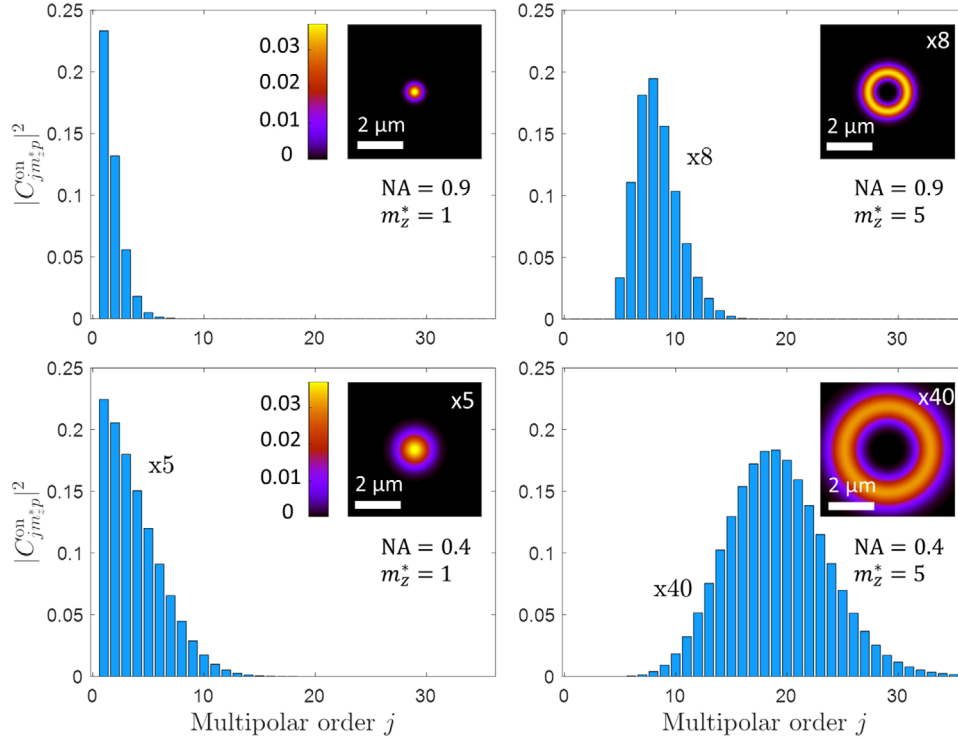
ADVANCED
SCIENCE NEWS

www.advancedsciencenews.com

LASER
& PHOTONICS
REVIEWS

www.lpr-journal.org

Figure 3. Beam shape function $|C^{\text{on}}_{j,m_z^*,p}|^2$ for NA = 0.9, 0.4 and $m_z^* = 1, 5$. The insets are $|\mathbf{E}^i|^2$ plots (in arbitrary units) of $6 \times 6\ \mu m^2$ at the focal plane $z = 0$. The axis and the scalebar of the insets are referred to the values of the plot for NA = 0.9 and $m_z^* = 1$. To make them comparable, the values of the other plots are multiplied by 5, 8, and 40, respectively. The $|\mathbf{E}^i|^2$ plots are normalized to 1.

with a certain NA, an increase in the AM content of the beam (m_z^*) widens the multipolar composition and displaces it toward greater js. This can also be observed in Figure 3, if one compares the left column decompositions ($m_z^* = 1$) with the right ones ($m_z^* = 5$). As a result of these two facts, a tightly focused Gaussian beam with helicity $p = m_z^* = 1$ can be described with just a handful of multipoles (see top left decomposition in Figure 3).

Now, once we have obtained the expression of $C^{\text{on}}_{j,m_z^*,p}$ for our cylindrically symmetric beam, we displace it by a vectorial distance $\mathbf{d} = d\hat{\mathbf{d}}$. This displacement affects the beam-shape function $C^{\text{on}}_{j,m_z^*,p}$. As a result, we obtain a new beam-shape function $C^{\text{off},\mathbf{d}}_{j,m_z^*,p} = C^{\text{off},\mathbf{d}}_{j,m_z,p}(C^{\text{on}}_{j,m_z^*,p}, \mathbf{d})$, and then we can rewrite Equation (4) as

$$\mathbf{E}^i(\mathbf{d}) = \sum_{j=1}^{\infty} \sum_{m_z=-j}^{j} C^{\text{off},\mathbf{d}}_{j,m_z,p} \left(\mathbf{A}^{(e)}_{jm_z} + p\mathbf{A}^{(m)}_{jm_z} \right) \tag{5}$$

where $C^{\text{off},\mathbf{d}}_{j,m_z,p}$ is computed as [21]

$$C^{\text{off},\mathbf{d}}_{j,m_z,p} = \sum_{n=-\min(j,j')}^{\min(j,j')} \sum_{L=0}^{\infty} (2L+1)(-i)^L j_L(kd)$$

$$\times \langle j, n; L, 0 | j', n \rangle \langle j, p; L, 0 | j', p \rangle$$

$$\sum_{j'=m_z^*}^{\infty} D^j(\hat{\mathbf{d}})_n^{m_z} D^{j'}(\hat{\mathbf{d}})_n^{m_z^*} C^{\text{on}}_{j'm_z^*p} \tag{6}$$

with $j_L(kd)$ being the spherical Bessel function; $\langle j_1, m_1; j_2, m_2 | J, M \rangle$ a Clebsch–Gordan coefficient; and $D^j(\hat{\mathbf{r}})_n^m$ being the Wigner matrix. Equations (5) and (6) show us that: i) Even if the initial beam was cylindrically symmetric, that is, it was an eigenstate of J_z with value m_z^*, the displaced beam generally is not. ii) The helicity of the beam p is maintained. The underlying reason is that the helicity operator Λ and the translation operator $T_{\mathbf{d}}$ commute. A significant particular case of Equations (5) and (6) is a translation along the symmetry axis z. In this case, due to the fact that J_z and T_z commute, the AM content is also conserved and Equations (5) and (6) become

$$\mathbf{E}^i(d\hat{\mathbf{z}}) = \sum_{j=m_z^*}^{\infty} C^{\text{off},d\hat{\mathbf{z}}}_{jm_z^*p} \left(\mathbf{A}^{(e)}_{jm_z} + p\mathbf{A}^{(m)}_{jm_z} \right)$$

$$C^{\text{off},d\hat{\mathbf{z}}}_{jm_z^*p} = \sum_{j'=m_z^*}^{\infty} C^{\text{on}}_{j'm_z^*p} \sum_{L=0}^{\infty} (2L+1)(-i)^L j_L(kd)$$

$$\times \langle j, n; L, 0 | j', n \rangle \langle j, p; L, 0 | j', p \rangle \tag{7}$$

2.2. Particular Case: Gaussian Beam Displaced along the y Axis

Up until this point, the theoretical treatment has been valid for any cylindrically symmetric beam. In the rest of the article, we study the case of a left circularly polarized Gaussian beam which is focused with a MO with a given NA at a distance $\mathbf{d} = d\hat{\mathbf{y}}$ from the center of the sphere. As explained before, the on-axis focused
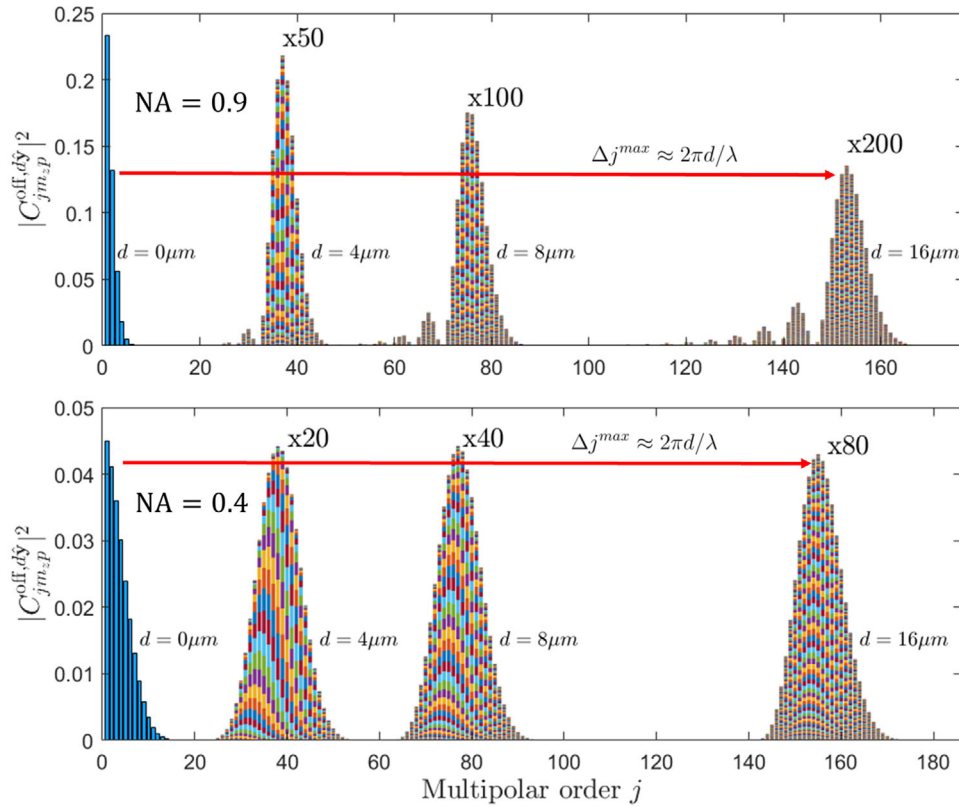
ADVANCED
SCIENCE NEWS

www.advancedsciencenews.com

LASER
& PHOTONICS
REVIEWS

www.lpr-journal.org

Figure 4. In blue, for both top and bottom subfigures, $|C_{j,m_z^*,p}^{on}|^2$ for NA = 0.9, 0.4. In many stacked colors, also for top and bottom subfigures, displaced beam-shape function $|C_{j,m_z,p}^{off,d\hat{y}}|^2$ for NA = 0.9, 0.4 and $d = 4, 8, 16$ μm. The $|C_{j,m_z,p}^{off,d\hat{y}}|^2$ distributions are multiplied by a number to make them comparable to the values of $|C_{j,m_z^*,p}^{on}|^2$. The incident nondisplaced beam (blue distribution) is obtained for a left circularly polarized Gaussian beam at $\lambda = 640$ nm.

beam is an eigenstate of Λ and J_z with eigenvalues $p = 1$, and $m_z^* = 1$, respectively.[25–27] We focus our attention in this case, as this is the typical experimental configuration that some of the authors have used in the past to excite WGMs in similar systems.[15–19] To be more precise, the polarization is not circular in the works in refs. [15–19]. Yet, the polarization state of the beam does not affect our analysis because we are dealing with displacements which are much larger than the wavelength. First of all, let us see how the multipolar decomposition of an on-axis Gaussian beam is modified due to d. This is depicted in **Figure 4** for two different NA values, NA = 0.9 (top row) and NA = 0.4 (bottom row). In both cases, we observe the on-axis decompositions $C_{j,m_z^*,p}^{on}$ depicted in Figure 3 on the left side of the plot. To their right, at higher multipolar orders j, we find some similar distributions corresponding to $C_{j,m_z,p}^{off,d\hat{y}}$ for different displacements d. We see that the off-axis distribution is built as an addition of lots of tiny contributions (represented by different colors). This is because, as shown by Equations (5) and (6), unlike the on-axis beam which has $m_z^* = p = 1$, the off-axis beam is obtained as a superposition of multipoles with different m_z values. Furthermore, we see that the off-axis multipolar decompositions $C_{j,m_z,p}^{off,d\hat{y}}$, if compared with $C_{j,m_z^*,p}^{on}$, are displaced toward greater js. In fact, one can see that the displacement is approximately linearly proportional to d. That is, let us define j_{max} as the multipolar order j at which a certain beam-shape function has its maximum value

$|C_{j,m_z,p}^{off,d}|$. Then we see that $\Delta j_{max} = j_{max}^{off,d\hat{y}} - j_{max}^{on} \approx 2\pi d/\lambda$. Now, remember that as it has been mentioned before, a WGM is a resonant mode with $q = 1$, and a large j, and $m = j$. As is seen both in Figures 3 and 4, an on-axis Gaussian beam cannot excite a WGM because its beam-shape function $C_{j,m_z^*,p}^{on}$ only has contributions from the lowest multipolar orders. Thanks to Figure 4, we realize that a displacement such as $\mathbf{d} = d\hat{y}$ tailors the beam-shape function $C_{j,m_z^*,p}^{on}$ and allows for the creation of arbitrarily large multipolar components. That is, to excite a WGM of order j with a Gaussian beam, we just need to displace it a distance of the order $d \approx j\lambda/2\pi$. Yet, this displacement by itself, does not guarantee that $q = 1$ and that $m = j$. In fact, Figure 4 shows that lots of different azimuthal modes (around the z axis) would be excited by these off-axis Gaussian beams. This is the case because the off-axis beam-shape function $C_{j,m_z,p}^{off,d}$ is composed of many m_z contributions for each j-multipolar subspace. Hence, the off-axis beam will excite a WGM with a large j and $m_z = j$, but it will also excite many other modes with the same j but with $m_z \neq j$. Note that the resonances of a sphere are degenerated in m_z, that is, all the modes with equal j but with different m_z share the same resonance. As a result, the pattern of the WGM $(j, m_z = j)$ will be hidden by the effect of all the rest of modes with $(j, m_z \neq j)$. Here, it is important to note that our theoretical multipolar description uses the z axis as the quantization axis. This choice is motivated by the fact that a circularly polarized Gaussian beam

**ADVANCED
SCIENCE NEWS**

www.advancedsciencenews.com

LASER
& PHOTONICS
REVIEWS

www.lpr-journal.org

propagating along the z axis is an eigenstate of J_z with value $|m_z^*| = 1$. However, it is clear that the $d\hat{y}$ displacement breaks the cylindrical symmetry along the z axis. In fact, because the displacement is done in the y direction, and the Gaussian beam also carries a certain linear momentum along the z axis P_z, it is intuitive to see that the off-axis Gaussian beam will necessarily carry some AM along the x axis of the initial frame of reference located at the center of the sphere. Thus, it might be useful to rewrite the off-axis beam-shape function $C_{j,m_z,p}^{\text{off},\mathbf{d}}$ as a function of m_x, instead of m_z. In fact, given our excitation scheme (see Figure 1), we observe that the off-axis configuration excites WGMs that revolve around the x axis, that is, $m = m_x$. This is also the case for the experimental works seen in the literature.[15–19] A WGM that revolves around the z axis would be perpendicular to the propagation direction of the incident beam (see Figure 1 to see the geometry of the problem). Mathematically, the Wigner matrix allows us to change from $C_{j,m_z,p}^{\text{off},d\hat{y}}$ to $C_{j,m_x,p}^{\text{off},d\hat{y}}$[21]

$$C_{j,m_x,p}^{\text{off},d\hat{y}} = \sum_{m_z=-j}^{j} d^j(-\pi/2)_{m_z}^{m_x} C_{j,m_z,p}^{\text{off},d\hat{y}} \tag{8}$$

where $d^j(\beta)_{m'}^m$ is the reduced Wigner matrix.[30] See the Supporting Information for the derivation of Equation (8). As a result of the change of basis done via Equation (8), we can rewrite the off-axis focused Gaussian beam as

$$\mathbf{E}^{i}(d\hat{y}) = \sum_{j=1}^{\infty} \sum_{m_x=-j}^{j} C_{j,m_x,p}^{\text{off},d\hat{y}} \left(\mathbf{A}_{jm_x}^{(e)} + p\mathbf{A}_{jm_x}^{(m)}\right) \tag{9}$$

$$C_{j,m_x,p}^{\text{off},d\hat{y}} = \sum_{n=-\min(j,j')}^{\min(j,j')} \sum_{L=0}^{\infty} (2L+1)(-i)^L j_L(kd)$$

$$\times \langle j,n;L,0|j',n\rangle\langle j,p;L,0|j',p\rangle \tag{10}$$

$$\sum_{j'=m_z^*}^{\infty} \sum_{m_z=-j}^{j} d^j(-\pi/2)_{m_z}^{m_x} D^j(\hat{\mathbf{d}})_n^{m_z} D^{j'}(\hat{\mathbf{d}})_n^{m_z^*} C_{j'm_z^*p}^{\text{on}}$$

Now, let us plot $C_{j,m_x,p}^{\text{off},d\hat{y}}$ for NA = 0.4 and $d = 0, 4, 8, 16$ μm as in Figure 4. Unlike Figure 4, where many colors indicate that the beam-shape function has many m_z components, **Figure 5** shows very few colors, meaning that each j-multipolar subspace is composed of very few m_x modes. Moreover, not only there are very few modes, but also the few modes that contribute to the decomposition are those with large m_x: the blue color indicates $m_x = j$, the yellow color means $m_x = j - 1$, etc. That is, the appearance of the WGM with $(j, m_x = j)$ will not be hidden under the the appearance of any other modes with $(j, m_x \neq j)$. Thus, thanks to the semi-analytical calculation of the beam-shape function, we have proven that a Gaussian beam propagating in the z direction which is displaced in the y axis by a distance d can efficiently excite WGMs of an order $j \approx 2\pi d/\lambda$ which revolve around the x axis with $m_x = j$.

The next step is proving that such an off-axis Gaussian beam can *efficiently* excite WGMs with $q = 1$. For doing this, we will have to deal with the beam-sphere interaction, as the efficiency
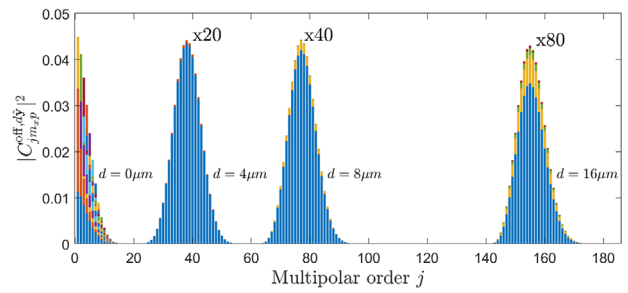

Figure 5. Displaced beam-shape function $|C_{j,m_x,p}^{\text{off},d\hat{y}}|^2$ for the rotated multipoles $\mathbf{A}_{jm_x}^{(y)}$. The plots are done for NA = 0.4 and $d = 0, 4, 8, 16$ μm. The blue color displays the weight of the multipolar modes with $m_x = j$, the yellow color shows the weights of $m_x = j - 1$, etc. The plot with $d = 0$ μm corresponds to the on-axis beam-shape function with $m_z^* = 1$. In all plots the wavelength is $\lambda = 640$ nm.

and the radial (or root) number q are parameters that stems from that interaction. Within Mie theory, $q = 1, \ldots, \infty$ is known as the radial (or root) number.[1,31–35] It is a number that enumerates the resonances of a certain Mie coefficient from low to high energy. That is, take the Mie coefficient $a_j(x)$, where x is the size parameter of the problem $x = 2\pi R/\lambda$, with R being the size of the particle, and λ the excitation wavelength. Note that the size parameter is proportional to the energy or frequency of the beam. There is a numerable infinite amount of frequencies $\{\omega_{j,q}^{(e)}\}$ that make $|a_j(\omega_{j,q}^{(e)})| = 1$. The set of frequencies $\{\omega_{j,q}^{(e)},\}$, which are the real part of the complex poles of $a_j(x)$, are such that $\omega_{j,q=1}^{(e)} < \omega_{j,q=2}^{(e)} < \ldots \omega_{j,q=n}^{(e)}$.[35,36] The reason why WGMs are typically defined as modes with $q = 1$ is because the Q-factor of the set $\{\omega_{j,q}^{(y)}\}$ decreases with q. That is, $\omega_{j,q=1}^{(y)}$ is the frequency that has the largest Q-factor among the whole $\{\omega_{j,q}^{(y)}\}$ set. These frequency sets have two more interesting properties. If $j > j'$, then i) Q-factor($\omega_{j,q=1}^{(y)}$) > Q-factor($\omega_{j',q=1}^{(y)}$), and ii) $\omega_{j,q=1}^{(y)} > \omega_{j',q=1}^{(y)}$. All these properties also hold for the sets of size parameters $\{x_{j,q}^{(e)}, x_{j,q}^{(m)}\}$. Now, let us assume that we excite at a certain λ a homogeneous sphere defined by (R, n_r), that is, its radius is R, and its relative index of refraction with respect to the embedding medium is n_r. Given these parameters, it will not be possible to excite WGMs of an order which is higher than $j^* \gtrsim 2\pi R/\lambda$.[11,14] That is a consequence of the fact that the size parameter of the problem, $x_p = 2\pi R/\lambda$ will be such that $x_{j^*-1,q=1}^{(y)} < x_p < x_{j^*,q=1}^{(y)} < x_{j^*+1,q=1}^{(y)}$. Depending on the laser, we might be able to tune the wavelength for a broader or a narrower interval. As a result, we might be able to have $x_p = x_{j^*,q=1}^{(y)}$, but it is clear that there will always be a $x_{j^*+1,q=1}^{(y)}$ that will be greater than the greatest possible experimental x_p. In conclusion, given a laser with λ and a particle with (R, n_r), the WGMs that can be excited will always have a $j \leq j^* \gtrsim 2\pi R/\lambda$. Of course, due to the fact that if $j > j'$, then Q-factor($x_{j,q=1}^{(y)}$) > Q-factor($x_{j',q=1}^{(y)}$), we will be especially interested in exciting the WGMs whose $j \lesssim j^* \gtrsim 2\pi R/\lambda$. Now the question is how to *efficiently* do it. For example, let us assume that $R = 8$ μm, and that $n_r = 1.45$. The wavelength is $\lambda = 640$ nm. As mentioned before, the greatest orders of WGMs that can be excited for this particle are of the order of $j^* \gtrsim 2\pi R/\lambda \approx 79$. Therefore, let us
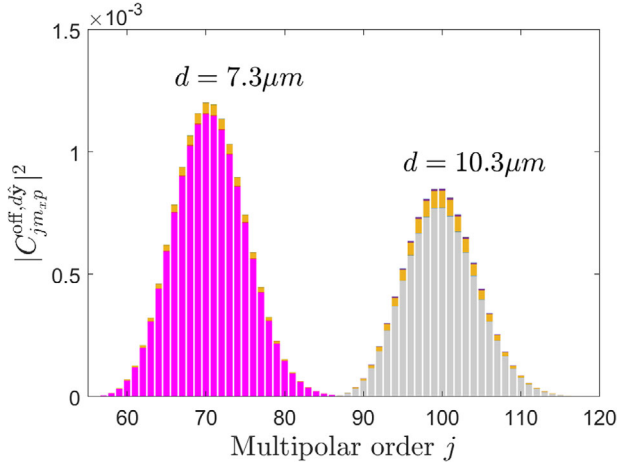
**ADVANCED
SCIENCE NEWS**

www.advancedsciencenews.com

LASER
& PHOTONICS
REVIEWS

www.lpr-journal.org

Figure 6. Displaced beam-shape function $|C^{\text{off},d\hat{y}}_{j,m_x,p}|^2$ in the rotated multipolar basis $\mathbf{A}^{(y)}_{jm_x}$ for $d = 7.3, 10.3$ μm. In all plots NA = 0.4, and $\lambda = 640$ nm. The incident beam is a left circularly polarized Gaussian beam.

take $j^* = 87$. We have seen that the condition to excite a j^*-order WGM at its $q = 1$ resonance is only a matter of size parameter matching, that is, $x_p = x^{(y)}_{j^*,q=1}$. But it is well known that a plane wave (or an on-axis Gaussian beam) with a wavelength such that the size parameter is $x_p = x^{(y)}_{j^*,q=1}$ will not excite this $j^* = 87$-order WGM. As shown in Figures 4 and 5, the underlying reason is that the beam-shape function of the incoming beam $C^{\text{off},d}_{j,m_z,p}$ must have some non-negligible components in the j^* multipolar order. In Figure 4, we have shown that this is achievable by displacing a Gaussian beam a distance $d \approx j^* \lambda/2\pi \approx 8$ μm from the center of the sphere. Figures 4 and 5 show that the beam-shape function of a Gaussian beam focused with an NA = 0.4 and displaced 8 μm from the center of the sphere has non-negligible contributions in the j=65–90 multipolar orders, and the maximum is at $j = 77$. This is in agreement with the approximation that d needs to be $d \approx j^* \lambda/2\pi \approx 8$ μm. The question arises: Given the experimental parameters $(R, n_r, \lambda, \text{NA})$, which displacement d maximizes the coupling efficiency to a WGM of order $j^* = 87$ (with $m = j^*$ and $q = 1$)? In **Figure 6**, we show that the displacement will need to be within the range $d = [7.3\text{–}10.3]$ μm. This can be inferred from the fact that $C^{\text{off},d\hat{y}}_{j,m_x,p}$ for $d = 7.3$ μm and $d = 10.3$ μm are non-negligible for $j \in [57, 87]$ and $j \in [87, 117]$ respectively.

These d-limits approximately correspond to two limit physical situations: $d = 7.3$ μm corresponds to the case where the beam is approximately tangential to the surface of the sphere from the inside, whereas $d = 10.3$ μm is the case where the beam is approximately tangential to the surface from the outside (see **Figure 7**). The case of $d = 8$ μm is the case where the center of the off-axis beam is tangential to the surface of the sphere. Next, we mathematically show that the most efficient off-axis configuration to excite a WGM is the outer tangential case. Yet, the displacement found is not $d = 10.3$ μm, but rather $d = 9.7$ μm. The reason has to do with the behaviour of Mie coefficients. Given a certain size parameter x, it exists a certain $j^* \gtrsim x$ such that both the Mie coefficients $a_j(x), b_j(x) = 0$ for $j \geq j^*$. At the same time, and for the same

size parameter x, the rest of Mie coefficients $a_j(x), b_j(x) \neq 0$ when $j < j^*$. We would like to excite the WGM associated to $j^* = 87$, which needs to be done at $x^{(y)}_{j^*=87,q=1}$. As a result, all Mie coefficients with $j < 87$ will be greater than zero at $x^{(y)}_{j^*=87,q=1}$. Now, ideally, we would like to excite a pure WGM of $j^* = 87$. Exciting a pure mode means that this is the only mode that is excited. If we look at Figures 6 and 7, we observe that the multipolar distributions associated to $d = 7.3, 8$ μm yield modes with $j < 87$. Thus, because the Mie coefficients $a_{j<87}(x^{(y)}_{j=87,q=1}), b_{j<87}(x^{(y)}_{j=87,q=1}) \neq 0$, the scattering will be inevitably composed of all the multipolar orders with $j < 87$ and such that $C^{\text{off},d\hat{y}}_{j,m_x,p}$ is non-negligible. Thus, there is only one way to get rid of all these lower order modes that will introduce some noise into the response of the system and hide the behavior of the pure WGM: The off-axis beam-shape function $C^{\text{off},d\hat{y}}_{j,m_x,p}$ must be negligible for $j < 87$. In our example, this is achieved with $d = 10.3$ μm, that is, with a beam whose incidence is tangential from the outside of the surface of the sphere. The case were $d = 10.3$ μm could be an acceptable efficient coupling from an experimental point of view, yet it may not be the most efficient possible coupling. Our theory allow us to compute the distance d that maximizes the efficiency of the coupling. Maximizing the coupling efficiency (CE) means maximizing the amount of power that goes into the desired WGM mode, given by a certain j and parity (e) or (m). It can be computed as

$$\text{CE}^{(e)}_{j^*}(d) = \frac{|a_{j^*} \, C^{\text{off},d\hat{y}}_{j^*,m_x=j^*,p}|^2}{\sum_{j=1}^{\infty} \sum_{m_x=-j}^{j} |C^{\text{off},d\hat{y}}_{j,m_x,p}|^2 (|a_j|^2 + |b_j|^2)} \quad (11)$$

$$\text{CE}^{(m)}_{j^*}(d) = \frac{|b_{j^*} \, C^{\text{off},d\hat{y}}_{j^*,m_x=j^*,p}|^2}{\sum_{j=1}^{\infty} \sum_{m_x=-j}^{j} |C^{\text{off},d\hat{y}}_{j,m_x,p}|^2 (|a_j|^2 + |b_j|^2)} \quad (12)$$

In **Figure 8**a we plot both $\text{CE}^{(y)}_{j^*=87}$ for $(y) = (e), (m)$. The plot is done at two different wavelengths. That is, $\text{CE}^{(e)}_{j^*}(d)$ is computed at $\lambda^{(e)}_{j^*=87} = 649.490$ nm, whereas $\text{CE}^{(m)}_{j^*}(d)$ is computed at $\lambda^{(m)}_{j^*=87} = 652.690$ nm. That is because, as mentioned above, each WGM has its own root number. And in this example, we have kept $R = 8$ μm. Figure 8a shows that $\text{CE}^{(e)}_{j^*}$ and $\text{CE}^{(m)}_{j^*}$ have their absolute maxima at $d = 9.7$ μm and $d = 9.6$ μm, respectively. For these d's, both $\text{CE}^{(y)}_{j^*}$ are greater than 90%. That is, almost all the energy that is coupled to particle is coupled to the targeted WGM: the efficiency of the coupling is almost perfect. Of course, $\text{CE}^{(y)}_{j^*}$ does not say anything about the absolute power coupled to WGM. That could be computed as

$$P^{(e)}_{j^*}(d) \propto |a_{j^*} \, C^{\text{off},d\hat{y}}_{j^*,m_x=j^*,p}|^2 \quad (13)$$

$$P^{(m)}_{j^*}(d) \propto |b_{j^*} \, C^{\text{off},d\hat{y}}_{j^*,m_x=j^*,p}|^2 \quad (14)$$

We have plotted $P^{(e)}_{j^*}$ in Figure 8b. We observe that the maximum power coupled to the targeted WGM $(j^* = 87)$ happens for $d = 9$ μm, which is not the d corresponding to the most efficient
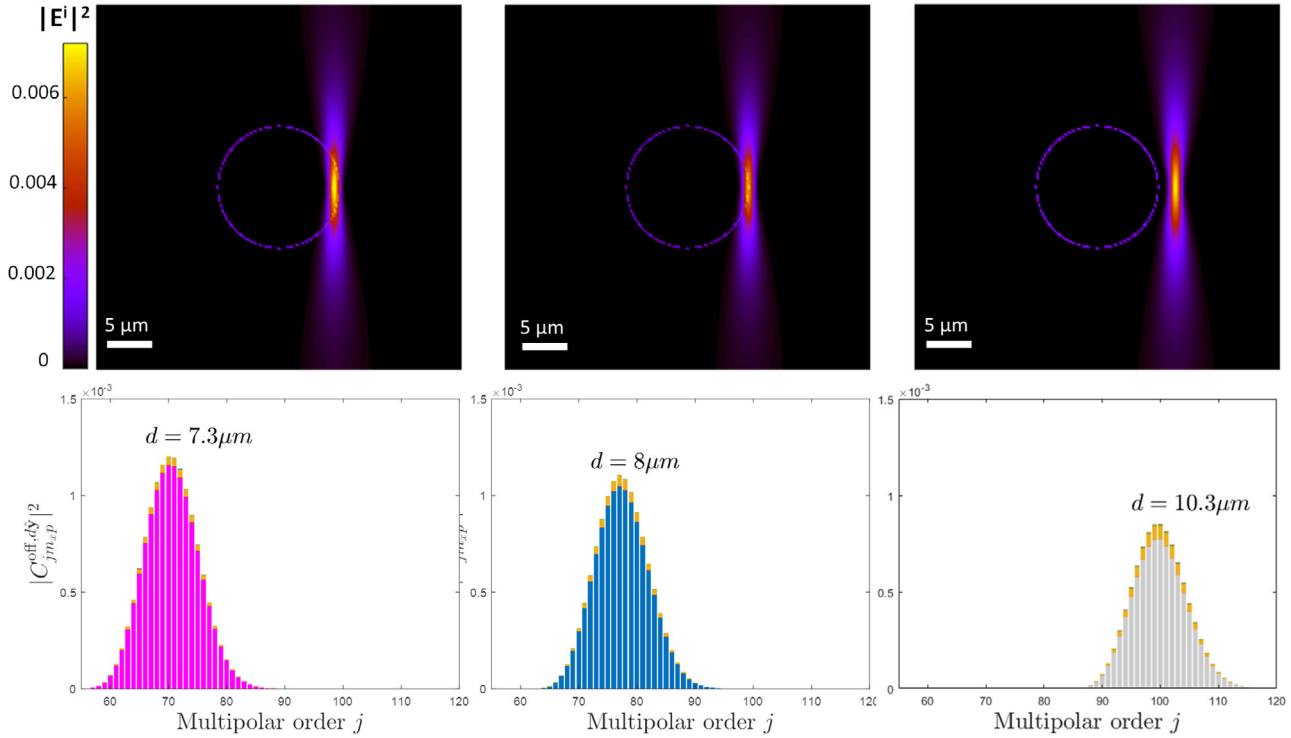
**ADVANCED
SCIENCE NEWS**

www.advancedsciencenews.com

**LASER
& PHOTONICS
REVIEWS**

www.lpr-journal.org

Figure 7. In the top row, plots of $|E^i|^2$ (in arbitrary units) for $d = 7.3, 8, 10.3$ μm in the $x = 0$ plane. The purple circumference shows the surface of a sphere of $R = 8$ μm. In the bottom row, plots of the displaced beam-shape function $|C^{off,d\hat{y}}_{j,m_x,p}|^2$ in the rotated multipolar basis $A^{(y)}_{jm_x}$ for the corresponding top row E^i fields with $d = 7.3, 8, 10.3$ μm. In all plots, NA = 0.4, and $\lambda = 640$ nm. The $|E^i|^2$ plots are normalized to 1.

coupling scenario. That is, for $d = 9$ μm, the power coupled into the WGMs of $j^* = 87$ is maximum, yet the purity of the targeted WGM is clearly lower with respect to the case with $d = 9.7$ μm. Note that in Figure 8b we have only plotted $P^{(e)}_{j^*}$, as $P^{(m)}_{j^*}$ yields the exact same values. This is because $|a_{87}(x^{(e)}_{87})| = |b_{87}(x^{(m)}_{87})| = 1$.

For completeness, in **Figure 9**a we plot the scattering cross section σ^{sca} for a sphere with $R = 8$ μm and $n_r = 1.45$ as a function

of $\lambda = [635, 655]$ nm for a left circularly polarized Gaussian beam displaced by $d = 9.7$ μm. Then, in Figure 9b we plot the total field $E^{tot} = E^i + E^{int} + E^{sca}$ at the $x^{(e)}_{87}$ resonant condition. Note that the coupling is so efficient that the intensity of the internal field is greater than that of the incident beam.

3. Conclusions

To wrap up, our analytical treatment has allowed us to describe the problem and predict the efficient excitation of WGMs with large j^*, $m = j^*$ and $q = 1$ with off-axis focused Gaussian beams. In particular, we have observed that:
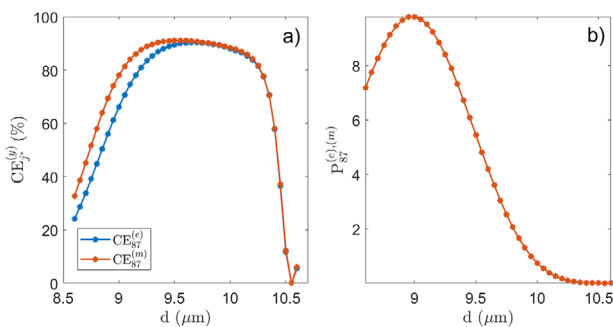

Figure 8. a) Coupling efficiency as a function of displacement of the incident beam d for the electric and magnetic resonances of $j^* = 87$. The blue line is computed for $x^{(e)}_{j^*=87} = 77.39$, whereas the red line is computed for $x^{(m)}_{j^*=87} = 77.01$. b) $P^{(y)}_{j^*=87}$ for both electric and magnetic modes. The two curves superimpose, as both $|a_{j^*=87}| = |b_{j^*=87}| = 1$ for their respective resonances $x^{(e)}_{87}$ and $x^{(m)}_{87}$. For both (a) and (b), the sphere is defined by $R = 8$ μm and $n_r = 1.45$, while the left circularly polarized Gaussian beam has NA = 0.4 and $\lambda = 640$ nm.

- The off-axis displacement d allows for the excitation of WGMs whose order j^* is proportional to d.
- The condition $m = j^*$ is immediately fulfilled for an m around the axis orthogonal to the plane defined by the directions of the beam propagation and the displacement. For instance, if the beam propagates along the z axis, and the displacement is in the y axis, then the relation $m = m_x = j^*$ is fulfilled.
- Experimentally, given a particle with (R, n_r), a tunable laser is needed in order to excite the j^*-WGM at its root number $q = 1$. A smart choice for the j^*-order of the WGM is $j^* \gtrsim 2\pi R / \lambda$, where λ is the central wavelength of the tunable laser. In this case, a narrowband tuning laser will do the job, since $x^{(y)}_{j^*,q=1} \approx 2\pi R / \lambda$, and as a result the resonant wavelength $\lambda^{(y)}_{j^*,q=1}$ will be approximately equal to the central wavelength of the laser λ.
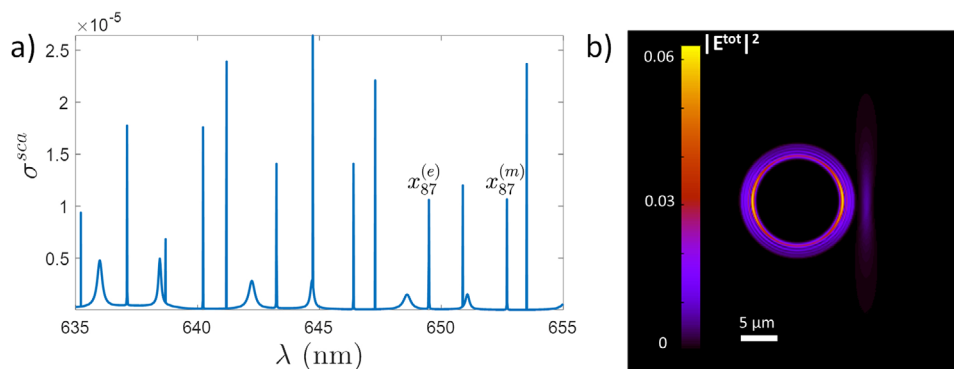
Figure 9. a) Scattering cross section σ^{sca} for 635 nm $\leq \lambda \leq$ 655 nm. The resonances used in Figure 8 are explicitly shown. b) Excitation of a WGM of the (e) kind with $j = 87$ and $m_x = j$. The plot shows $|\mathbf{E}^{tot}|^2$ (in arbitrary units) for an area of 48×48 μm² in the $x = 0$ plane. In all the plots, $R = 8$ μm, $n_r = 1.45$, and the displaced left circularly polarized Gaussian beam has NA $= 0.4$ and $d = 9.7$ μm. The incident field $|\mathbf{E}^i|^2$ is normalized to 1.

- The efficiency of the coupling can be computed and maximized as a function of the displacement parameter d. The most efficient coupling always happens for beams whose intensity distribution is mainly located outside (yet almost tangentially) of the surface of the sphere.

We have also seen that four interactions regimes can be sketched as a function of the position of the incident beam with respect to the surface of the sphere. The nature of these four interaction regimes is purely geometrical, and as a result their numerical definition depends on λ, d, R, n_r, NA. Last but not least, contrary to the current state-of-the-art description of the problem, we have observed that the coupling of a propagating beam onto a WGM is not a product of any evanescent tunnelling. The coupling is produced via scattering due to an AM matching of the targeted WGM and the content of the off-axis incident beam.

Supporting Information

Supporting Information is available from the Wiley Online Library or from the author.

Acknowledgements

Conflict of Interest

The authors declare no conflict of interest.

Data Availability Statement

Data sharing is not applicable to this article as no new data were created or analyzed in this study.

[1] A. N. Oraevsky, *Quantum Electron.* **2002**, *32*, 377.
[2] G. Gouesbet, G. Gréhan, *Generalized Lorenz-Mie Theories*, Springer, Berlin **2011**.
[3] J. P. Barton, D. R. Alexander, S. A. Schaub, *J. Appl. Phys.* **1989**, *65*, 2900.
[4] G. Gouesbet, J. A. Lock, *J. Opt. Soc. Am. A* **1994**, *11*, 2516.
[5] J. A. Lock, *J. Opt. Soc. Am. A* **1998**, *15*, 2986.
[6] J. A. Lock, *Opt. Lett.* **1999**, *24*, 427.
[7] A. Serpengüzel, S. Arnold, G. Griffel, *Opt. Lett.* **1995**, *20*, 654.
[8] A. Serpengüzel, S. Arnold, G. Griffel, J. A. Lock, *J. Opt. Soc. Am. B* **1997**, *14*, 790.
[9] X. Zambrana-Puyalto, X. Vidal, G. Molina-Terriza, *Opt. Express* **2012**, *20*, 24536.
[10] X. Zambrana-Puyalto, G. Molina-Terriza, *J. Quant. Spectrosc. Radiat. Transfer* **2013**, *126*, 50.
[11] X. Zambrana-Puyalto, *Ph.D. Thesis*, Macquarie University **2014**.
[12] A. Aiello, P. Banzer, M. Neugebauer, G. Leuchs, *Nat. Photonics* **2015**, *9*, 789.
[13] I. Fernandez-Corbaton, X. Zambrana-Puyalto, N. Bonod, C. Rockstuhl, *Phys. Rev. A* **2016**, *94*, 053822.
[14] X. Zambrana-Puyalto, X. Vidal, M. L. Juan, G. Molina-Terriza, *Opt. Express* **2013**, *21*, 17520.
[15] R. Zullo, A. Giorgini, S. Avino, P. Malara, P. De Natale, G. Gagliardi, *Opt. Lett.* **2016**, *41*, 650.
[16] A. Giorgini, S. Avino, P. Malara, P. De Natale, G. Gagliardi, *Sci. Rep.* **2017**, *7*, 41997.
[17] A. Giorgini, S. Avino, P. Malara, P. De Natale, G. Gagliardi, *Opt. Lett.* **2018**, *43*, 3473.
[18] A. Giorgini, S. Avino, P. Malara, P. De Natale, M. Yannai, T. Carmon, G. Gagliardi, *Phys. Rev. Lett.* **2018**, *120*, 073902.
[19] A. Giorgini, S. Avino, P. Malara, P. De Natale, G. Gagliardi, *Sensors* **2019**, *19*, 473.
[20] M. E. Rose, *Multipole Fields*, Wiley, New York **1955**.
[21] W.-K. Tung, *Group Theory in Physics*, World Scientific, Singapore **1985**.

[22] J. D. Jackson, *Classical Electrodynamics: Third Edition*, John Wiley & Sons, New York **1999**.

[23] C. F. Bohren, D. R. Huffman, *Absorption and Scattering of Light by Small Particles*, Wiley science paperback series. Wiley, Hoboken, NJ **1983**.

[24] N. Tischler, I. Fernandez-Corbaton, X. Zambrana-Puyalto, A. Minovich, X. Vidal, M. L. Juan, G. Molina-Terriza, *Light: Sci. Appl.* **2014**, *3*, e183.

[25] X. Zambrana-Puyalto, X. Vidal, G. Molina-Terriza, *Nat. Commun.* **2014**, *5*, 4922.

[26] X. Zambrana-Puyalto, X. Vidal, I. Fernandez-Corbaton, G. Molina-Terriza, *Sci. Rep.* **2016**, *6*, 22185.

[27] X. Zambrana-Puyalto, X. Vidal, P. Woźniak, P. Banzer, G. Molina-Terriza, *ACS Photonics* **2018**, *5*, 2936.

[28] I. Fernandez-Corbaton, X. Zambrana-Puyalto, G. Molina-Terriza, *Phys. Rev. A* **2012**, *86*, 042103.

[29] L. Novotny, B. Hecht, *Principles of Nano-Optics*, Cambridge University Press, Cambridge **2006**.

[30] S. Stoll, A. Schweiger, *J. Magn. Reson.* **2006**, *178*, 42.

[31] S. Schietinger, O. Benson, *J. Phys. B: At., Mol. Opt. Phys.* **2009**, *42*, 114001.

[32] V. R. Dantham, P. B. Bisht, *J. Opt. Soc. Am. B* **2009**, *26*, 290.

[33] L. Deych, J. Rubin, *Phys. Rev. A* **2009**, *80*, 061805.

[34] J. Rubin, L. Deych, *Phys. Rev. A* **2010**, *81*, 053827.

[35] X. Zambrana-Puyalto, N. Bonod, *Phys. Rev. B* **2015**, *91*, 195422.

[36] V. Grigoriev, S. Varault, G. Boudarham, B. Stout, J. Wenger, N. Bonod, *Phys. Rev. A* **2013**, *88*, 063805.